Electronic Supplementary Information (ESI):

Rapid synthesis of self-supported three-dimensional bubble-like graphene frameworks as high-performance electrodes for supercapacitors

*Haiyan Duan,‡ Tingting Yan,‡ Zhenying Li, Guorong Chen, Jianping Zhang, Liyi Shi, Dengsong Zhang**

Research Center of Nano Science and Technology, Shanghai University, Shanghai 200444, China.

Fax: 86 21 66136079; E-mail: dszhang@shu.edu.cn

‡ *These authors contributed equally to this work.*

Experimental Section

For comparision, the compact traditional graphene (TGR) was also successfully prepared. Firstly, graphite oxide (GO) was fabricated via the Hummers' method.[1] Then the dried GO powders were thermally reduced at 300 ^{o}C for about 2 min in a tubular furnace to obtain TGR products.

The density of 3DGF and GC electrode is calculated according to the following formula:

$$\rho = \frac{m}{v} = \frac{m}{s \bullet h} \qquad \text{(S1)}$$

By using S1 formula, the density of the electrode material is calculated: 0.30 g cm^{-3} for 3DGF and 1.40 g cm^{-3} for GC.

The reaction mechanism of photopolymerization

The nanocomposite polymers can be obtained in few seconds by photopolymerization at room temperature. The detailed reaction mechanism is as follows: Active ions are firstly generated when the photoinitiator is activated by absorbing UV radiation energy, which will interact with the unsaturated group and epoxy group of epoxy acrylate resin and 1,4-butanediol diglycidyl ether. These generated active groups can also interaction. Thus, the chain transfer reactions are initiated and nanocomposite polymers are rapidly achieved.

Supplementary experimental results

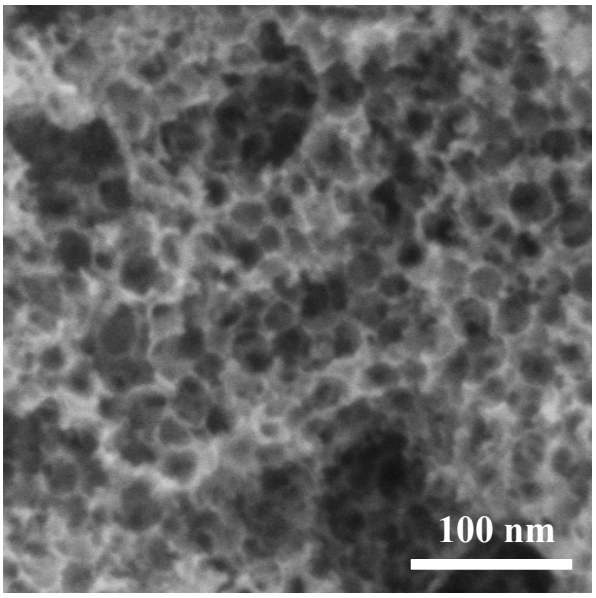

Fig. S1 SEM images of 3DGF.

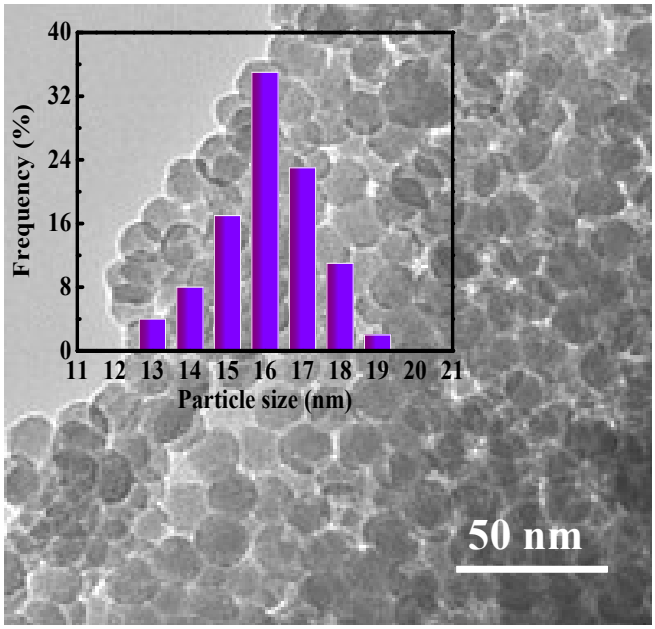

Fig. S2 TEM images and the corresponding particle size distribution histograms of silica-16nm.

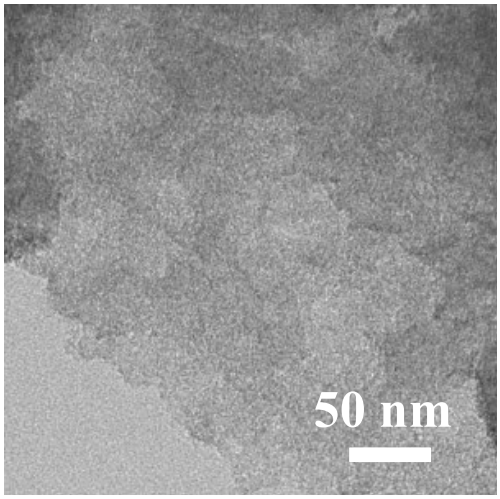

Fig. S3 TEM images of GC.

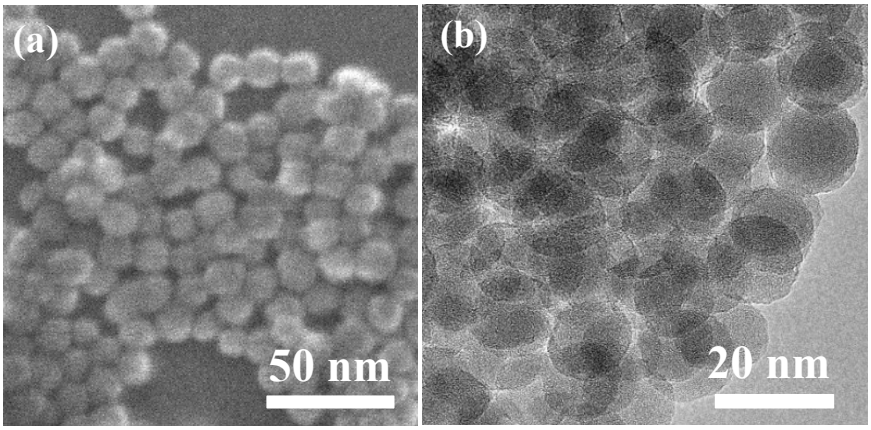

Fig. S4 (a) SEM and (b) TEM images of nanocomposite polymers.

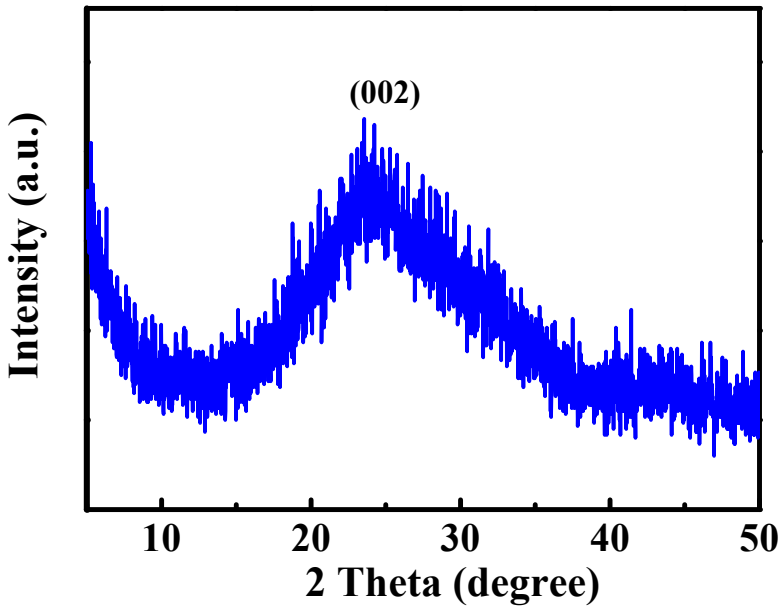

Fig. S5 XRD patterns of the TGR.

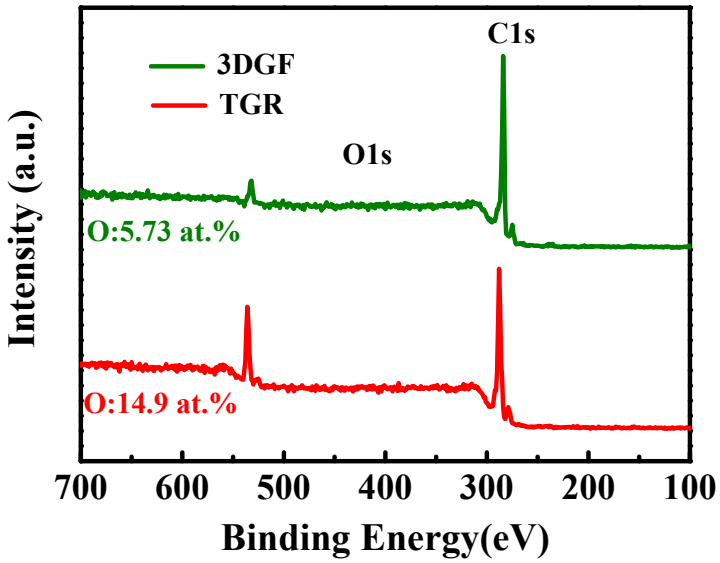

Fig. S6 XPS survey scan spectra of the 3DGF and the TGR.

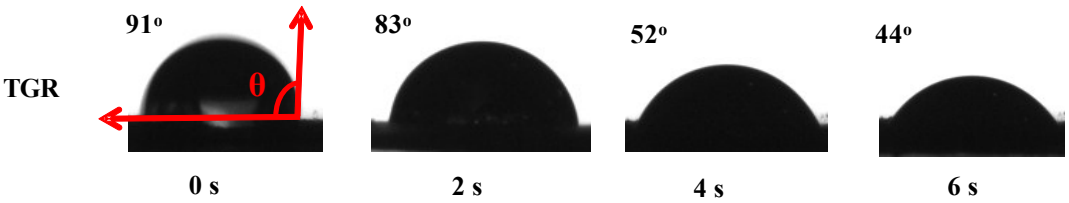

Fig. S7 Optical micrographs of the water contact angles on the surface of TGR as a function of contact time.

The speed of the disappearance of the droplet on the surface of electrodes was driven by adsorption and/or spreading, which may result from the following aspects: (1) The interactions between the water molecular and the oxygen-containing groups. (2) The hydrophobicity/hydrophilicity of the nature of the carbon materials which can influenced by abundant porous structures and specific surface area. The richer porous structures are in favor of the adsorption onto the porous materials. (3) The effect of porosity (like capillary effects) of the materials. The richer porosity can be beneficial to the adsorption onto the porous materials. The dynamic contact angles measurements of the TGR are presented in Fig.S7. It should be noted that the contact angle of TGR decreased rather slowly as time goes on, suggesting the characteristic of highly hydrophobic. The initial contact angle of TGR is 91 °, then down to 44° after 6 s. They are much larger than that of 3DGF with rich 3D interconnected porous networks and porosity.

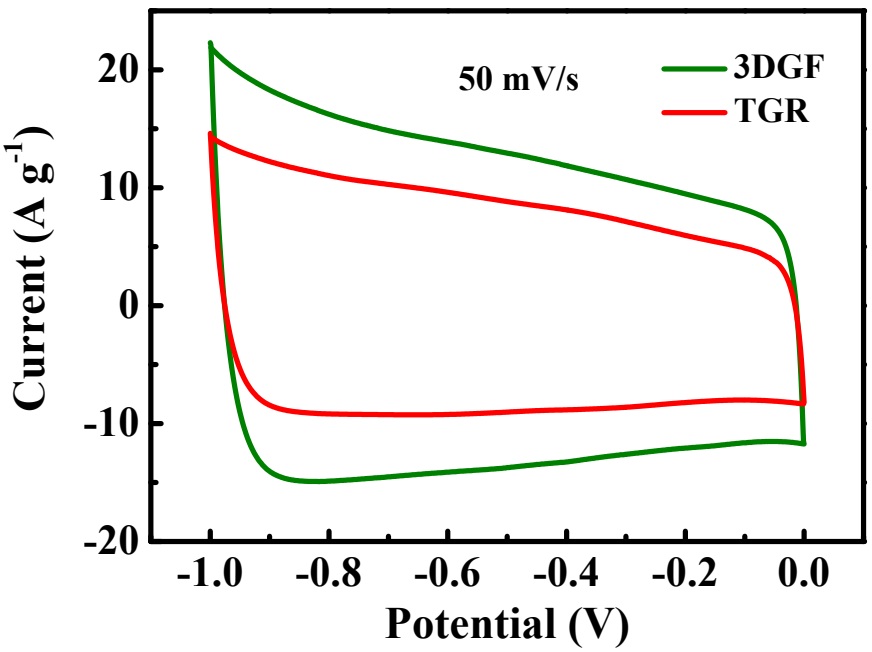

Fig. S8 CV curves of TGR and 3DGF at a scan rate of 50 mV s^{-1}.

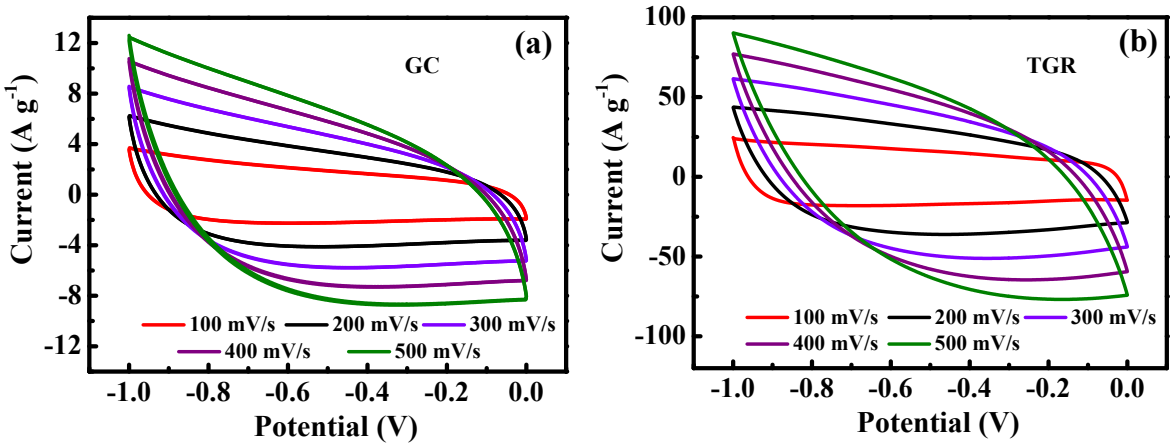

Fig. S9 CV curves of GC and TGR at different scan rates from 100 to 500 mV s^{-1}.

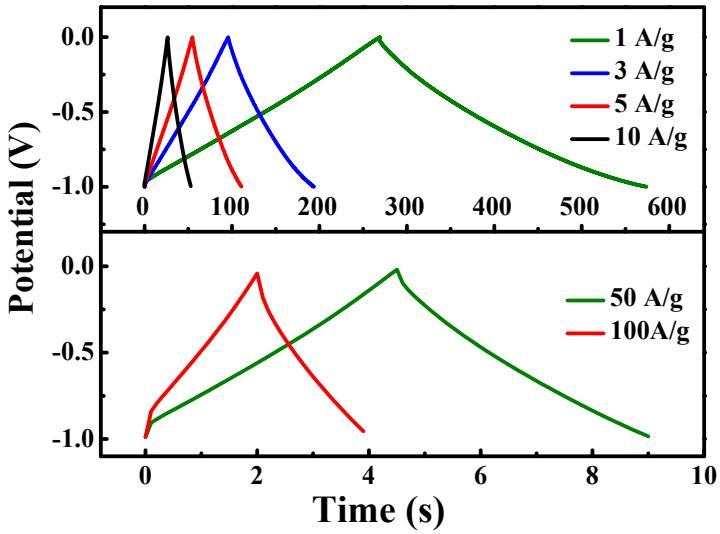

Fig. S10 CP curves of the 3DGF in a 6 M KOH solution at different current densities.

Table S1 Comparison of rate performances of carbon-based electrodes from the literature.

Electrode materials	Current density	Rate performance	
		References	**3DGF (This work)**
Activated carbon	0.1-15 A g^{-1}	16[2]	**78**
Hollow carbon nanospheres	0.1-15 A g^{-1}	71[2]	**78**
Nitrogen-doped ordered nanoporous carbons	0.1-10 A g^{-1}	50[3]	**81**
3D micro-porous conducting carbon beehive	0.5-10 A g^{-1}	71[4]	**83**
Carbon nanocages	0.1-10 A g^{-1}	68[5]	**81**
Carbon nanocages	10-100 mV s^{-1}	74[5]	**88**
Porous nitrogen-doped hollow carbon spheres	0.5-10 A g^{-1}	56[6]	**83**
Nanoporous carbon	5-50 mV s^{-1}	78[7]	**90**
3D N-doped graphene-CNT networks	0.5-10 A g^{-1}	53[8]	**83**
Nitrogen-enriched nonporous carbon	0.05-10 A g^{-1}	71[9]	**81**
Hierarchical nitrogen-doped carbon nanocages	1-100 A g^{-1}	75[10]	**82**
3D strutted graphene	1-100 A g^{-1}	52[11]	**82**

Table S2 Comparison of capacitance and detailed information on the mass loading of various carbon electrode materials from the literature.

Electrode materials	Electrolyte	Mass loading for each electrode	Current Density [A g^{-1}]	Capacitance [F g^{-1}]
Thin-sheet carbon nanomesh	6M KOH	1.4 mg cm^{-2}	1	160[12]
Hollow carbon nanospheres	6M KOH	---	10	~160[2]
Soya derived heteroatom doped carbon	1M H_2SO_4	~2 mg	10	140[13]
N-doped porous carbon nanofibers	6M KOH	5.0-6.0 mg cm^{-2}	1	202[14]
N-enriched carbon from melamine-mica	6M KOH	2.0-7.0 mg cm^{-2}	1	198[9]
Mesoporous graphene frameworks	1M H_2SO_4	0.89 mg cm^{-2}	1	190[15]
ZIF-derived porous carbon	6M KOH	5 mg cm^{-2}	10	178[16]
Nitrogen doped carbon nanotube	1 M H_2SO_4	0.35 mg cm^{-2}	1	~160[17]
Hierarchical porous carbon	6M KOH	----	1	196[18]
Milled strutted graphene	1 M H_2SO_4	1 mg	1	~180[11]
Hierarchically ordered mesoporous carbon/graphene	6M KOH	0.5-2.0 mg cm^{-2}	10	194[19]
Graphene films	6M KOH	----	1	175[20]
Activated carbon	6M KOH	----	10	~120[21]
Carbonaceous nanoflasks	6M KOH	2.5 mg cm^{-2}	1	222[22]
3DGF	6M KOH	2.0-5.0 mg cm^{-2}	1	277 (This work)
3DGF	6M KOH	2.0-5.0 mg cm^{-2}	10	262 (This work)

References

1. D. Zhang, T. Yan, L. Shi, Z. Peng, X. Wen and J. Zhang, *J Mater Chem,* 2012, **22**, 14696-14704.
2. F. Xu, Z. Tang, S. Huang, L. Chen, Y. Liang, W. Mai, H. Zhong, R. Fu and D. Wu, *Nat. Commun,* 2015, **6**, 7221-7230.
3. Y. Liang, H. Liu, Z. Li, R. Fu and D. Wu, *J Mater Chem A,* 2013, **1**, 15207-15211.
4. P. Dhanya, V. Aravindan, M. Srinivasan and S. Ogale, *Energy Environ. Sci,* 2013, **7**, 728-735.
5. K. Xie, X. Qin, X. Wang, Y. Wang, H. Tao, Q. Wu, L. Yang and Z. Hu, *Adv Mater,* 2012, **24**, 347-352.
6. J. Han, G. Xu, B. Ding, J. Pan, H. Dou and D.R. Macfarlane, *J Mater Chem A,* 2014, **2**, 5352-5357.
7. B. Liu, H. Shioyama, T. Akita and Q. Xu, *J. Am. Chem. Soc,* 2008, **130**, 5390-5391.
8. B. You, L. Wang, L. Yao and J. Yang, *Chem. Commun,* 2013, **49**, 5016-5018.
9. H.J. Denisa, K. Masaya, S. Soshi, H. Hiroaki, Z.H. Zhu and G.Q. Lu, *Adv. Funct. Mater,* 2009, **19**, 1800-1809.
10. J. Zhao, H. Lai, Z. Lyu, Y. Jiang, K. Xie, X. Wang, Q. Wu, L. Yang, Z. Jin, Y. Ma, J. Liu and Z. Hu, *Adv Mater,* 2015, **27**, 3541-3545.
11. X. Wang, Y. Zhang, C. Zhi, X. Wang, D. Tang, Y. Xu, Q. Weng, X. Jiang, M. Mitome, D. Golberg and Y. Bando, *Nat. Commun,* 2013, **4**, 2905-2912.
12. H. Wang, L. Zhi, K. Liu, L. Dang, Z. Liu, Z. Lei, C. Yu and J. Qiu, *Adv. Funct. Mater,* 2015, **25**, 5420-5427.
13. M. Rana, K. Subramani, M. Sathish and U.K. Gautam, *Carbon,* 2017, **114**, 679-689.
14. X.-D.Z. Li-Feng Chen, Hai-Wei Liang, Mingguang Kong, Qing-Fang Guan, Ping Chen, and a.S.-H.Y. Zhen-Yu Wu, *ACS Nano,* 2012, **6**, 7092-7102.
15. L. Ji, G. Guo, H. Sheng, S. Qin, B. Wang, D. Han, T. Li, D. Yang and A. Dong, *Chem. Mater,* 2016, **28**, 3823-3830.
16. P. Zhang, F. Sun, Z. Shen and D. Cao, *J Mater Chem A,* 2014, **2**, 12873-12880.
17. D. Gueon and J.H. Moon, *ACS Appl Mater. Inter,* 2015, **7**, 20083-20089.
18. D. Jia, X. Yu, H. Tan, X. Li, F. Han, L. Li and H. Liu, *J. Mater. Chem. A,* 2017, **5**, 1516-1525.
19. Y. Song, Z. Li, K. Guo and T. Shao, *Nanoscale,* 2016, **8**, 15671-15680.
20. B. Z, Z. W, M. W, W. Z, S. X, C. J, Y. J, W. Z, C. K and F. X, *Adv Mater,* 2013, **25**, 5799-5806.
21. J. Cui, Y. Xi, S. Chen, D. Li, X. She, J. Sun, W. Han, D. Yang and S. Guo, *Adv. Funct. Mater,* 2016, **26**, 8487-8495.
22. C. Chen, H. Wang, C. Han, J. Deng, J. Wang, M. Li, M. Tang, H. Jin and Y. Wang, *J. Am. Chem. Soc,* 2017, **139**, 2657-2663.